JUSAN SCIENCE

Journal of Engineering and Environmental Systems

ISSN (Print): 3135-2510; ISSN (Online): 3135-2529

journal homepage: https://jusanscience.com/journals/jees

Research Article

Comparative Study of Ag and Cu Decorated Mesoporous Silica Nanoparticles for Adsorptive Desulfurization of Dibenzothiophene

Aigerim Ospanova*, Aliya Kurbanova

Renewable Energy Laboratory, National Laboratory Astana (NLA), Nazarbayev University, Kabanbay Batyr 53, Astana 010000, Kazakhstan

Corresponding author: Aigerim Ospanova a.ospanova@nu.edu.kz

https://doi.org/10.66973/jees.26.009

Article info:

Received: 13 May 2026 / Revised: 10 June 2026 / Accepted: 11 June 2026 / Published: 11 June 2026

Ospanova, A., Kurbanova A. (2026). Comparative Study of Ag and Cu Decorated Mesoporous Silica Nanoparticles for Adsorptive Desulfurization of Dibenzothiophene. *Journal of Engineering and Environmental Systems*, 1(1), 111–127. https://doi.org/10.66973/jees.26.009

Abstract: Mesoporous SiO_2 nanoparticles and metal-decorated silica nanocomposites (SiO_2–Ag and SiO_2–Cu) were synthesized and evaluated for the adsorptive removal of dibenzothiophene (DBT) from model fuel solutions. The structural and morphological properties of the synthesized materials were investigated using Fourier transform infrared spectroscopy (FTIR), X-ray diffraction (XRD) and transmission electron microscopy (TEM). TEM analysis confirmed the formation of spherical mesoporous silica nanoparticles with highly ordered pore structures, while Ag and Cu nanoparticles were successfully dispersed on the silica surface without significant destruction of the mesoporous framework. Adsorption experiments demonstrated that metal decoration significantly enhanced the initial adsorption rate of DBT, with SiO_2–Ag and SiO_2–Cu achieving removal efficiencies of 44.2% and 42.9%, respectively, after 30 min, compared with only 9.3% for pure SiO_2. However, pure mesoporous SiO_2 exhibited the highest final adsorption efficiency, reaching 90.6% after 24 h, whereas SiO_2–Ag and SiO_2–Cu achieved 80.4% and 80.6%, respectively. The superior long-term adsorption performance of pure SiO_2 was attributed to its highly accessible mesoporous structure and larger effective surface area, while Ag and Cu nanoparticles provided rapid initial adsorption through enhanced metal–sulfur interactions with DBT molecules. The results demonstrate the important relationship between adsorption kinetics and pore accessibility in mesoporous silica-based adsorbents for desulfurization applications.

Keywords: Mesoporous silica nanoparticles; Dibenzothiophene (DBT) adsorption; Fuel desulfurization; Silver-decorated silica; Copper-decorated silica; Sulfur removal; Adsorptive Desulfurization.

1 Introduction

The removal of sulfur-containing compounds from liquid fuels remains a critical challenge due to increasingly stringent environmental regulations and the need to reduce sulfur oxide emissions [1],

https://doi.org/10.66973/jees.26.009

[2]. Among refractory sulfur compounds, dibenzothiophene (DBT) and its derivatives are particularly difficult to eliminate because of their aromatic structure and steric hindrance [3], [4]. Conventional hydrodesulfurization (HDS), although widely employed in refineries, requires elevated temperatures and hydrogen pressures, resulting in high energy consumption and gradual catalyst deactivation. Consequently, adsorption-based desulfurization has emerged as a promising alternative due to its operational simplicity, lower energy requirements, and potential for selective sulfur removal under mild conditions [5], [6].

Mesoporous silica nanoparticles (MSNs) are attractive adsorbent platforms owing to their high specific surface area, ordered pore structure, tunable pore size distribution, and facile surface modification [7], [8]. Their well-defined mesoporous channels promote rapid diffusion of bulky sulfur compounds such as DBT while maintaining accessibility to active adsorption sites. However, pristine silica generally exhibits limited adsorption performance because DBT adsorption is primarily governed by weak van der Waals forces and hydrogen-bonding interactions associated with surface silanol groups [9].

To enhance adsorption performance, metal decoration of mesoporous silica has been widely explored. Incorporation of metal species such as silver and copper introduces specific adsorption sites capable of interacting with sulfur-containing molecules through π-complexation, hard-soft acid-base (HSAB) interactions, and coordinative binding mechanisms [10], [11]. Silver species are known to interact strongly with thiophenic sulfur compounds through π-complexation and soft acid-base interactions, whereas copper species can provide additional coordinative adsorption sites and strengthen sulfur–metal interactions. The adsorption efficiency depends strongly on metal identity, oxidation state, dispersion, and the nature of the metal–silica interface [12], [13], [14].

Surfactant-templated synthesis methods, such as CTAB-assisted sol–gel processes, enable the preparation of highly ordered MSNs with large accessible surface areas and uniform pore networks [15], [16]. Subsequent modification through reduction or wet impregnation allows controlled incorporation of metal nanoparticles or oxide species onto the silica framework. Despite numerous studies on metal-modified silica adsorbents, a direct comparison between Ag- and Cu-decorated mesoporous silica nanoparticles for DBT removal under identical experimental conditions remains limited [17], [18].

In this study, mesoporous silica nanoparticles were synthesized via a CTAB-templated sol-gel route and subsequently decorated with Ag and Cu to produce SiO_2-Ag and SiO_2-Cu materials. Adsorption experiments were conducted under standardized conditions to compare DBT removal efficiency and adsorption behavior. The objective is to elucidate how metal identity and surface chemistry influence DBT adsorption performance and to provide insights for the development of efficient adsorptive desulfurization materials.

2 Materials and Methods

2.1 Materials

Cetyltrimethylammonium bromide (CTAB), tetraethyl orthosilicate (TEOS), sodium hydroxide (NaOH), silver nitrate ($AgNO_3$), copper nitrate trihydrate ($Cu(NO_3)_2 \cdot 3H_2O$), sodium borohydride ($NaBH_4$), ethanol, and 3-aminopropyltriethoxysilane (APTES) were all purchased from Sigma-Aldrich (St. Louis, MO, USA) and used as received without further purification. Deionized water was used in all synthesis procedures.

2.2 Synthesis of Mesoporous SiO_2 Nanoparticles (MSN)

Mesoporous silica nanoparticles were synthesized via a CTAB-templated sol-gel method according to a previously reported procedure [19]. Briefly, 60 mg of CTAB was dissolved in 30 mL of deionized

https://doi.org/10.66973/jees.26.009

water under magnetic stirring at 75 °C. Subsequently, 300 µL of 2 M NaOH solution was added to adjust the pH and promote hydrolysis. After 5 min of stirring, 500 µL of tetraethyl orthosilicate (TEOS) was added dropwise to the solution under continuous stirring. The reaction was allowed to proceed for 2 h at 75 °C to form mesoporous silica nanoparticles. The resulting particles were collected by centrifugation, washed several times with deionized water and ethanol, dried at 60 °C overnight, and subsequently calcined at 550 °C for 4 h to remove the CTAB template and generate the mesoporous structure.

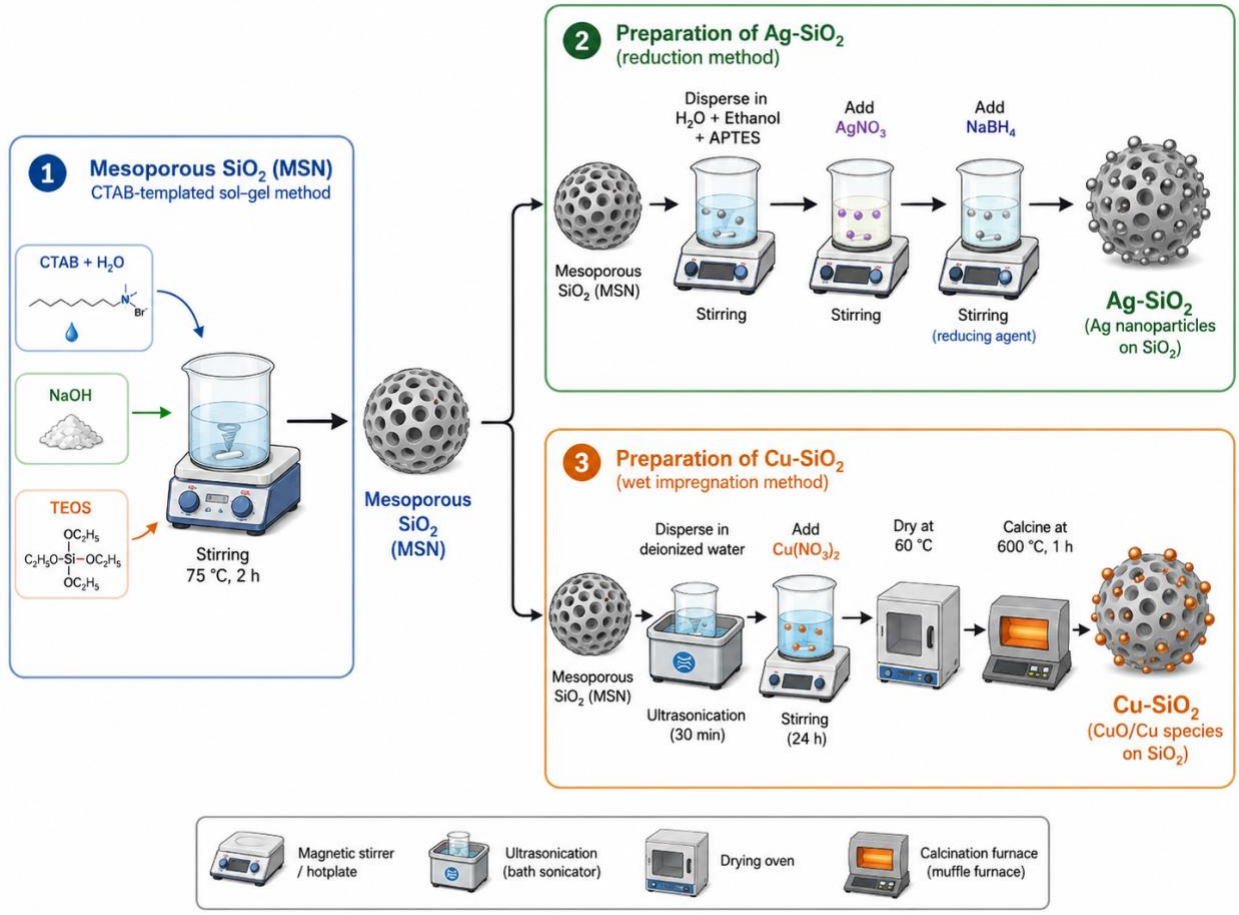

Figure 1. Schematic illustration of the synthesis of mesoporous SiO_2 nanoparticles (MSN) and th eir modification to Ag–SiO_2 and Cu–SiO_2.

2.3 Preparation of SiO_2-Ag via Reduction Method

Silver-decorated silica nanoparticles were prepared using an in situ reduction approach. First, 100 mg of mesoporous SiO_2 nanoparticles were dispersed in a mixture of 80 mL water, 2 mL ethanol, and 40 µL APTES and ultrasonicated for 30 min to functionalize the silica surface with amine groups. Subsequently, 10 mg silver nitrate ($AgNO_3$) was added and stirred for 30 min to allow adsorption of Ag^+ ions onto the functionalized silica surface.

Afterward, 200 µL of freshly prepared 0.1 M sodium borohydride ($NaBH_4$) solution was added dropwise as a reducing agent, and the mixture was stirred for an additional 5 min to reduce Ag^+ to metallic silver nanoparticles (Ag^0). The resulting SiO_2-Ag nanoparticles were collected by

https://doi.org/10.66973/jees.26.009

centrifugation, washed with water and ethanol to remove residual reagents, and dried at 60 °C.

2.4 Preparation of Cu-SiO_2 via Wet Impregnation Method

Copper-decorated silica nanoparticles were prepared using a wet impregnation technique. Mesoporous SiO_2 nanoparticles (100 mg) were first dispersed in 50 mL deionized water and ultrasonicated for 30 min to ensure uniform dispersion. Copper nitrate ($Cu(NO_3)_2$, 30 mg) was then added, and the mixture was stirred for 24 h to allow adsorption of copper ions onto the silica surface.

The solid was subsequently separated by centrifugation and dried at 60 °C. Finally, the material was calcined at 600 °C for 1 h in air to convert the copper precursor into copper oxide species anchored on the silica surface. The final product was denoted as Cu-SiO_2.

Figure 1 shows the stepwise synthesis of mesoporous SiO_2 nanoparticles using a CTAB-templated sol–gel method, followed by surface modification to prepare Ag–SiO_2 through the reduction method and Cu–SiO_2 through the wet impregnation method.

2.5 Characterization

The morphology and particle size of the synthesized nanoparticles were examined using transmission electron microscopy (TEM) **(**JEM 1400 Plus Jeol, Japan). The porous structure and dispersion of metal nanoparticles on the silica surface were evaluated to confirm successful synthesis and metal decoration.

The chemical structure and functional groups of the synthesized mesoporous silica nanoparticles were analyzed using a Nicolet iS5 FTIR spectrometer (Thermo Fisher Scientific, USA).

The structural properties and phase composition of the synthesized nanoparticles were investigated using X-ray diffraction (XRD, Rigaku Corp., Tokyo, Japan). XRD patterns were recorded using Cu Kα radiation (λ = 1.5406 Å) over a 2θ range of 10–80°.

2.6 Adsorption Experiments

Batch adsorption experiments were carried out by adding 20 mg of adsorbent to 20 mL of DBT solution in octane with an initial concentration of 60 mg L^{-1}. The mixture was stirred under controlled conditions, and aliquots were collected at predetermined time intervals. The residual DBT concentration was determined using UV–Vis spectroscopy (Spectrometer I - Evolution 300 (Thermo Scientific)), and the desulfurization efficiency was calculated based on the decrease in DBT concentration.

The removal efficiency was calculated using:

$$Removal\ efficiency(\%) = \frac{C_0 - C_t}{C_0} \times 100$$

3 Results and Discussion.

The adsorption behavior of dibenzothiophene over mesoporous SiO_2, SiO_2–Ag, and SiO_2–Cu nanoparticles exhibits a distinct trade-off between initial removal behavior and ultimate equilibrium capacity. This comparative study highlights the specific roles of structural accessibility and surface chemical interactions in the adsorptive desulfurization of liquid fuels [20].

Table 1 summarizes the effect of contact time on the adsorption performance of SiO_2, SiO_2–Ag, and SiO_2–Cu nanomaterials toward dibenzothiophene (DBT) removal. The residual DBT concentration and corresponding removal efficiency were monitored over a 24 h adsorption period to evaluate the adsorption behavior and time-dependent efficiency of the prepared nanocomposites. The obtained results demonstrate notable differences in

https://doi.org/10.66973/jees.26.009

adsorption kinetics and equilibrium removal efficiency among the investigated materials.

Table 1. Time-Dependent Adsorption Performance of SiO_2, SiO_2–Ag, and SiO_2–Cu Nanocomposites for Dibenzothiophene Removal

Time	**SiO_2**		**SiO_2-Ag**		**SiO_2-Cu**	
	C (ppm)	Removal efficiency (%)	C (ppm)	Removal efficiency (%)	C (ppm)	Removal efficiency (%)
0	59.30		59.30		59.30	
30 min	53.8	9.3	33.08	44.2	33.84	42.9
1 h	36.42	38.6	36.58	38.3	36.12	39.1
2 h	17.79	70.0	31.43	47.0	20.76	65.0
4 h	6.65	88.8	7.08	88.1	7.33	87.6
24 h	5.60	90.6	11.63	80.4	11.50	80.6

3.1. Equilibrium Adsorption and Structural Influence

Experimental results indicate that pure mesoporous SiO_2 provides the most efficient long-term removal, achieving a final adsorption efficiency of 90.6% after 24 hours. In contrast, the metal-modified variants, SiO_2–Ag and SiO_2–Cu, reached lower equilibrium removals of 80.4% and 80.6%, respectively. The superior capacity of unmodified silica is primarily attributed to its highly ordered mesoporous network and high specific surface area, which remain fully accessible for DBT molecules [20], [21]. Adsorption on pristine silica is largely driven by physical mechanisms, including van der Waals interactions between the aromatic rings of DBT and surface silanol groups, as well as unhindered pore diffusion within the internal channels [22].

The relative decrease in equilibrium capacity for the metal-decorated adsorbents likely stems from structural modifications during the impregnation or deposition processes. The incorporation of Ag and Cu nanoparticles can lead to partial pore blockage or a reduction in the effective surface area [23]. As observed in similar systems using template-assisted

https://doi.org/10.66973/jees.26.009

silica supports, excessive metal loading or poor dispersion can narrow pore apertures, thereby creating steric hindrance that limits the diffusion of bulky organosulfur molecules into the internal mesoporous network during prolonged contact periods [23], [24].

3.2 Kinetic Performance and Surface Interactions

While pure silica excels at equilibrium, the metal-decorated nanoparticles demonstrate significantly enhanced adsorption kinetics during the initial stages. After only 30 minutes, removal efficiencies for SiO_2–Ag and SiO_2–Cu reached 44.2% and 42.9%, respectively, whereas pure SiO_2 removed only 9.3%. This rapid initial uptake suggests that Ag and Cu species introduce highly active surface sites that facilitate immediate chemical interactions [21], [22].

The higher initial DBT removal observed for the modified samples may be associated with stronger interactions between DBT and the supported Ag-containing and copper oxide species. In SiO_2–Ag, Ag-containing sites may promote adsorption through Ag–S interactions and interactions with the π-electron system of DBT [22], [30]. In SiO_2–Cu, the CuO and possible minor Cu_2O species may interact with thiophenic sulfur through Cu–S coordination, Lewis acid–base interactions, and related donor–acceptor mechanisms [23], [24], [27]. These surface interactions may facilitate rapid DBT adsorption at external metal-containing sites and pore entrances before slower intraparticle diffusion becomes more influential.

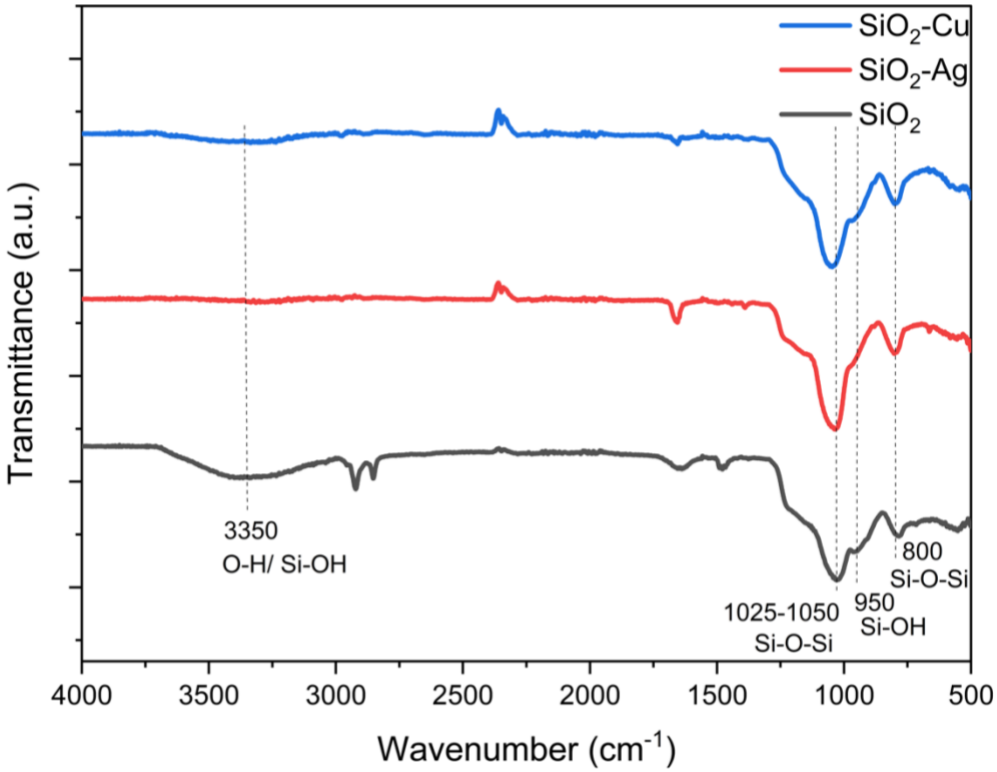

Figure 2. FTIR spectra of SiO_2, SiO_2–Ag and SiO_2–Cu.

3.3 Comparative Mechanisms and Desulfurization Pathways

The desulfurization performance follows a clear mechanistic transition:

https://doi.org/10.66973/jees.26.009

- Initial Phase (0–30 min): Adsorption is dominated by chemisorptive surface interactions on the Ag and Cu sites, favoring the metal-decorated materials.
- Equilibrium Phase (up to 24 h): As surface sites saturate, the process transitions to internal pore diffusion. The pure SiO_2 material, maintaining its open architectural integrity and high silanol density, eventually outperforms the modified variants by providing greater overall accessible volume for DBT sequestration [22], [24].

These findings suggest that while metal decoration is essential for applications requiring rapid sulfur removal (e.g., high-flow systems), maintaining the structural openness of the mesoporous support is critical for maximizing the total desulfurization capacity of the adsorbent. Future optimization could focus on achieving better metal dispersion through confined-space synthesis to mitigate pore blockage while retaining high kinetic activity [23].

FTIR analysis was performed to identify the characteristic functional groups of the synthesized mesoporous silica nanoparticles and to confirm the formation of the silica framework. As shown in Figure 2, the spectrum exhibited a broad absorption band in the region of 3200–3600 cm^{-1}, which can be attributed to the stretching vibration of surface hydroxyl groups and adsorbed water molecules.

The main characteristic bands of silica were observed at approximately 1050–1100, 950, and 800 cm^{-1}. The intense band around 1050–1100 cm^{-1} is assigned to the asymmetric stretching vibration of Si–O–Si bonds, confirming the formation of the silica network. The band near 800 cm^{-1} corresponds to the symmetric stretching vibration of Si–O–Si, while the band around 450–470 cm^{-1} is related to the bending vibration of Si–O–Si bonds. In addition, the weak band around 950–970 cm^{-1} can be attributed to the stretching vibration of surface silanol groups (Si–OH).

The absence or significant decrease of C–H stretching bands at approximately 2920 and 2850 cm^{-1} indicates the effective removal of the CTAB template. Overall, the FTIR results confirm the successful formation of mesoporous silica nanoparticles with characteristic Si–O–Si and Si–OH functional groups.

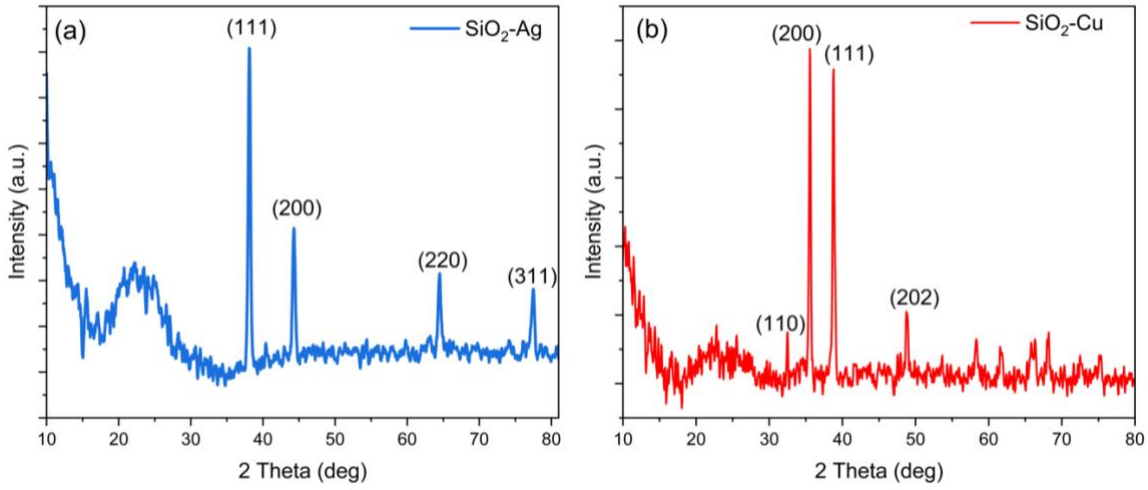

Figure 3. XRD patterns of SiO_2–Ag and SiO_2–Cu nanoparticles.

The X-ray diffraction patterns for the SiO_2–Ag and SiO_2–Cu nanoparticles provide critical data regarding the phase composition and structural integrity of the adsorbents used in dibenzothiophene sequestration (Figure 3).

https://doi.org/10.66973/jees.26.009

The X-ray diffraction (XRD) patterns of Ag- and Cu-decorated SiO_2 nanoparticles are shown in Figure 3. Both samples exhibit a broad diffraction band centered at ~20–25° (2θ), which is characteristic of amorphous silica, confirming that the mesoporous SiO_2 support retains its non-crystalline structure after metal loading and calcination. This behavior is consistent with previously reported silica-based nanocomposites. The SiO_2–Ag sample displays distinct diffraction peaks at approximately: ~38° (111); ~44° (200); ~64° (220); ~77° (311). These peaks correspond to the face-centered cubic (fcc) structure of metallic silver (Ag^0). The strong intensity of the (111) reflection indicates preferred crystallographic orientation, which is commonly observed in Ag nanoparticles due to its lowest surface energy plane. The presence of these crystalline silver phases is significant for desulfurization performance. These sites facilitate the rapid removal of DBT through π-complexation interactions, where the Ag(I) or metallic Ag species interact with the -electrons of the thiophenic rings and the sulfur atoms. The sharpness of the peaks indicates that the Ag species are successfully consolidated into crystalline clusters, which serve as the primary active sites for the enhanced initial adsorption kinetics [22], [26].

The X-ray diffraction (XRD) pattern of the Cu-decorated SiO_2 nanocomposite is shown in Figure 3 (b). A broad diffraction band centered at $2\theta \approx 22–23°$ is observed, which is characteristic of amorphous SiO_2, confirming that the silica support retains its non-crystalline structure after the impregnation and calcination processes. A weak diffraction peak located at approximately 29.6° (110) can be attributed to the cubic Cu_2O phase, suggesting that a fraction of copper species exists in the Cu^+ oxidation state. The relatively low intensity of this peak indicates that Cu_2O is a minor phase in the composite. The major diffraction peaks are observed at 35.5° (200); 38.7° (111); 49° (202). These reflections correspond to the monoclinic CuO (tenorite) structure, confirming that copper is predominantly present in the Cu^{2+} oxidation state. The presence of multiple CuO-related peaks demonstrates successful formation of crystalline CuO nanoparticles on the silica surface. The coexistence of both CuO and Cu_2O phases indicates a mixed-valence copper system, which may arise due to partial reduction of Cu^{2+} during synthesis or incomplete oxidation during calcination. However, the dominance of CuO peaks confirms that the thermal treatment in air favors the formation of the CuO phase as the thermodynamically stable oxide. The successful detection of these crystalline peaks confirms that the copper species have effectively d ispersed and bonded to the silica surface. These sit es provide the necessary electronic environment to form strong donor-acceptor complexes with organo sulfur compounds. The partial incorporation of the se species within the confined spaces of the mesop ores, as suggested by the relative peak intensities, h elps stabilize the active phase for repeated adsorpti on cycles. The integration of these XRD findings d emonstrates a synergistic material design. The amo rphous mesoporous silica serves as the architectura l platform, providing the large pore volume and int ernal surface area required for long-term equilibriu m capacity. Simultaneously, the crystalline metalli c phases identified in the patterns act as the kinetic accelerators. These transition metal sites provide hi gher binding energies for sulfur than the unmodifie d silanol groups, explaining why the metal-decorat ed variants achieve significantly higher DBT remo val efficiencies (over 40%) within the first 30 minu tes of the adsorption process [26], [27].

https://doi.org/10.66973/jees.26.009

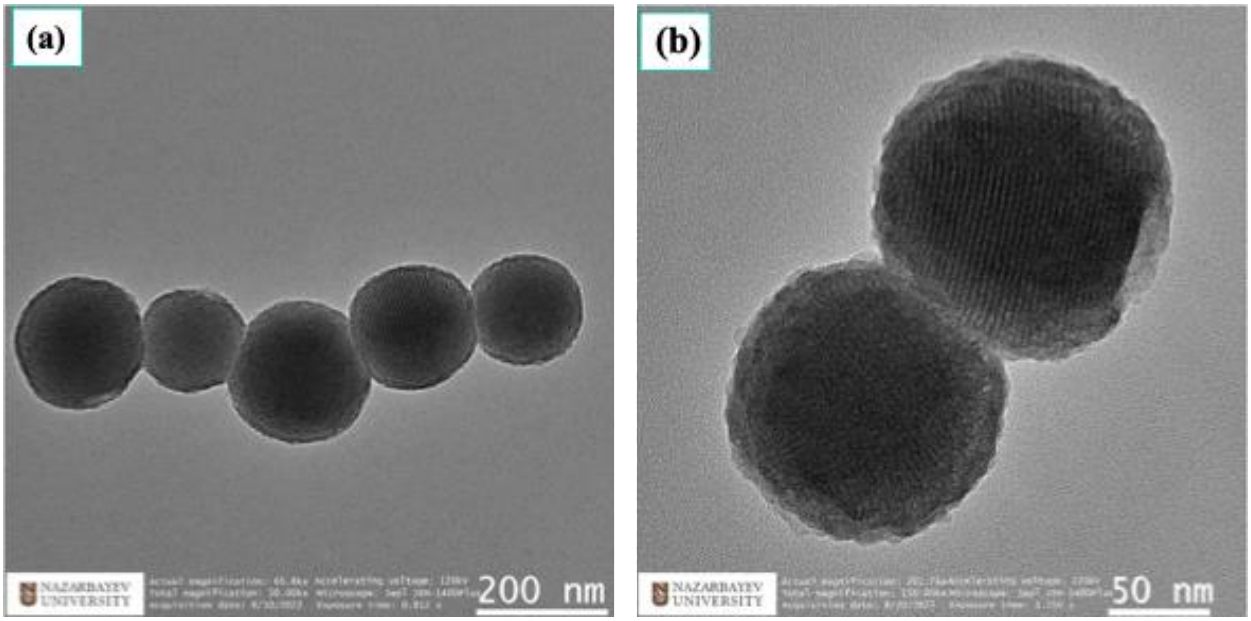

Figure 4. TEM images of mesoporous SiO_2 nanoparticles at different magnifications showing spherical morphology and ordered mesoporous structure.

The TEM analysis of the synthesized SiO_2 nanoparticles provides critical evidence regarding their morphological uniformity and internal structural order, both of which are fundamental to their performance in dibenzothiophene sequestration.

The TEM images (Figure 4) reveal the formation of well-dispersed, spherical nanoparticles characterized by a smooth external morphology and a nearly monodisperse size distribution. The absence of significant irregular aggregation indicates that the synthesis conditions—likely governed by controlled hydrolysis and condensation—successfully promoted homogeneous nucleation and restricted secondary growth. This spherical architecture is highly advantageous for liquid-phase adsorption, as it ensures a high surface-area-to-volume ratio and reduces the diffusion path length for adsorbate molecules compared to bulk or irregularly shaped materials. The uniformity observed in the diameters suggests excellent colloidal stability during the preparation phase, which is essential for maintaining consistent active site density in desulfurization applications [29].

TEM imaging in Figure 4 (b) elucidates the internal mesostructure, characterized by clearly visible ordered pore channels and periodic contrast patterns. These patterns confirm the successful formation of a mesoporous framework, often associated with hexagonal or cubic symmetries typical of high-performance silica adsorbents [20]. Such highly ordered architectures are strategically beneficial for DBT removal for several reasons:

- Accessible Surface Area: The internal porosity provides a massive specific surface area and an abundance of silanol groups, which serve as primary interaction sites for DBT through van der Waals forces and interactions [22].
- Diffusion Pathways: The straight, ordered channels act as efficient "molecular highways," facilitating rapid mass transfer and reducing the steric hindrance typically encountered by bulky organosulfur molecules during intraparticle diffusion [24].
- Structural Integrity: The robust silica framework maintains its pore accessibility even after

https://doi.org/10.66973/jees.26.009

functionalization with metals like Ag or Cu, provided the metal loading is optimized to prevent significant pore blockage [24].

The observed periodicity and spherical symmetry are consistent with established literature on mesostructured silica spheres used in deep desulfurization. These structural features ensure that the adsorbent provides not only a high equilibrium capacity but also reproducible kinetic profiles, making them suitable for the selective removal of organosulfur compounds from complex fuel matrices [24].

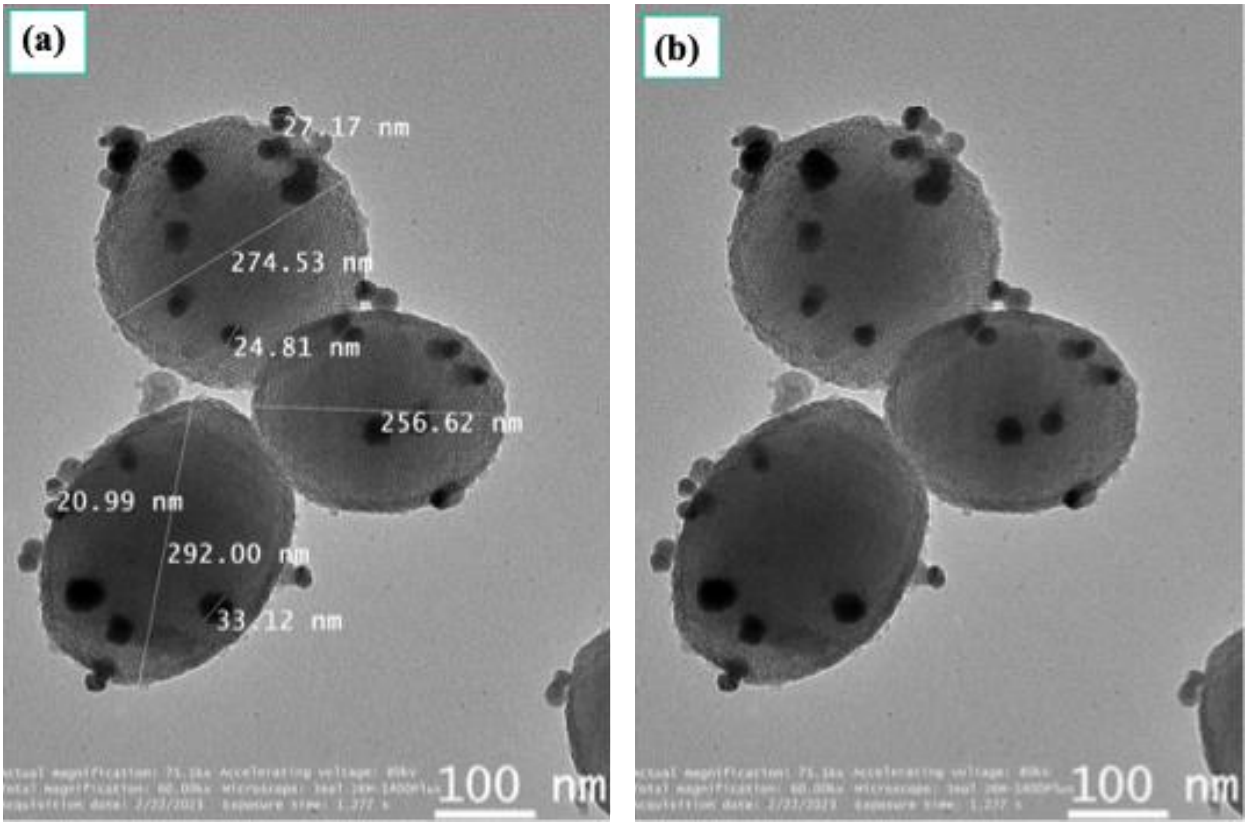

Figure 5. TEM images of Ag-decorated mesoporous silica nanoparticles (SiO_2–Ag) showing spherical mesoporous silica particles and surface-dispersed Ag nanoparticles.

https://doi.org/10.66973/jees.26.009

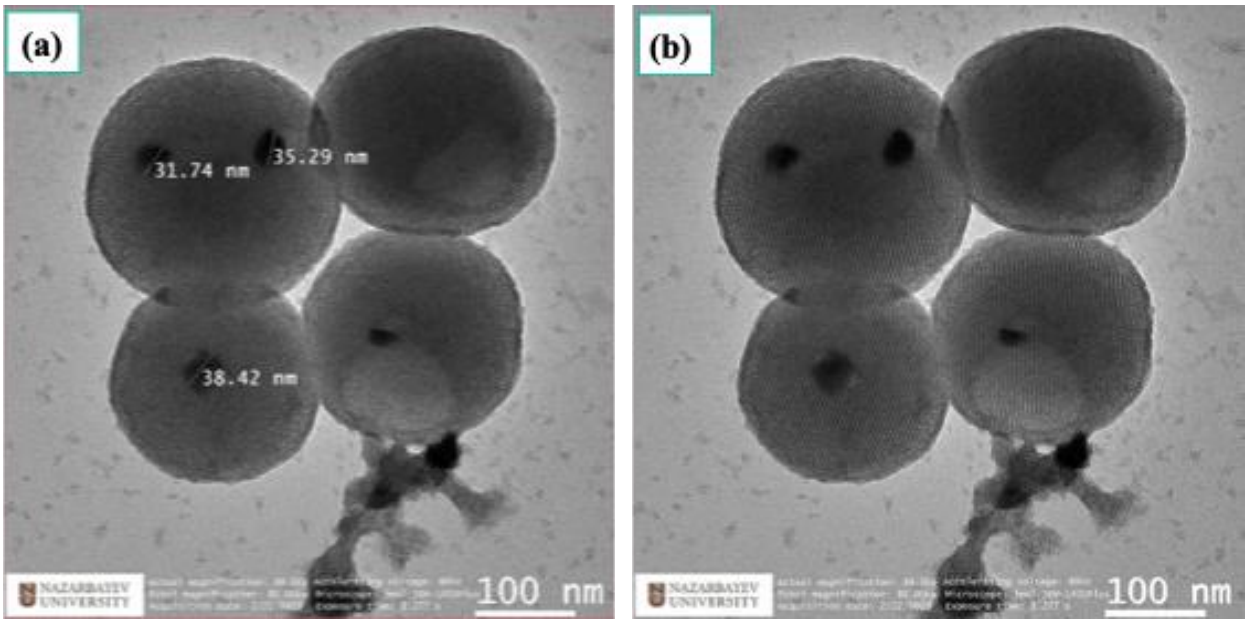

Figure 6. TEM images of Cu-decorated mesoporous silica nanoparticles (SiO_2–Cu) showing ordered mesoporous silica spheres and dispersed Cu nanoparticles on the silica surface.

The TEM analysis of the metal-decorated silica nanoparticles (SiO_2–Ag and SiO_2–Cu) confirms the successful immobilization of active metallic species while maintaining the high structural integrity of the mesoporous support. These morphological features are critical for balancing the requirements of high surface area and active site accessibility in the deep desulfurization of fuels [27].

1. Morphological and Structural Analysis of SiO_2–Ag

The TEM images of the SiO_2–Ag nanoparticles rev eal that the silica supports maintain a uniform sphe rical geometry with diameters ranging from 250 to 300 nm (Figure 5). The incorporation of silver doe s not disrupt the characteristic ordered mesostructu re, as well-defined periodic pore arrangements rem ain visible throughout the framework [21].

Dark-contrast particles, predominantly 20–35 nm i n size, were observed on the silica surface (Figure 5) and were tentatively assigned to Ag-containing s pecies based on their greater electron contrast relat ive to the SiO_2 matrix. These Ag nanoparticles are well-dispersed across the silica surface and a high degree of dispersion, achieved without severe aggr egation, is essential for maximizing the exposure o f Ag sites, which facilitate the rapid capture of DB T molecules via π-complexation [24]. The successf ul stabilization of these small Ag clusters is likely mediated by interactions with the abundant surface silanol groups during the synthesis process.

2. Morphological and Structural Analysis of SiO_2–Cu

Similarly, the SiO_2–Cu samples confirm the successful loading of copper-based species onto the mesoporous spheres (Figure 6). The silica matrix continues to exhibit highly ordered mesoporous channels and spherical morphology after Cu incorporation, indicating that the metal decoration protocol is non-destructive to the underlying framework [23].

Dark contrast regions, attributed to Cu nanoparticle s, are observed with sizes approximately between 3 0 and 40 nm. Notably, these Cu species appear bot h on the external surface and partially embedded w ithin the internal porous structure. Compared to the SiO_2–Ag system, the slightly lower density of visi

https://doi.org/10.66973/jees.26.009

ble surface particles in SiO_2–Cu may suggest that a significant fraction of the copper species is located within the confined spaces of the mesopores. While such internal dispersion can enhance the stability of the active sites, it also emphasizes the need for careful loading control to prevent the pore blockage that can limit the diffusion of bulky organosulfur molecules like DBT [23], [24].

3. Functional Implications for DBT Adsorption

The preservation of the ordered mesostructure in both modified materials is a vital finding. An intact porous network ensures that the large specific surface area of the silica support remains accessible, providing efficient diffusion pathways for DBT molecules [23].

The integration of Ag and Cu nanoparticles introduces a synergistic effect: the mesoporous silica provides the necessary structural platform for high-capacity sequestration, while the metallic nanoparticles offer highly active sites for metal–sulfur interactions. These interactions are responsible for the markedly improved adsorption kinetics observed during the initial stages of the process, as the high affinity between the transition metals and the sulfur atoms in DBT allows for immediate surface capture before intraparticle diffusion becomes the rate-limiting step. Consequently, these TEM observations provide a structural basis for the enhanced desulfurization performance of the metal-decorated adsorbents [22], [23], [24].

Proposed mechanism of DBT adsorption on SiO_2, SiO_2-Ag, and SiO_2-Cu nanoparticles

The removal of dibenzothiophene from model fuel using modified nanoparticles is driven by a synergistic combination of physical and chemical interactions. As illustrated in the proposed mechanism (Figure 7), the performance of these materials is governed by porous adsorption, surface silanol groups, and specific metal–sulfur affinities [22], [27].

1. Bare SiO_2: Physical Trapping and Surface Silanols

For bare mesoporous silica (SiO_2), the adsorption process is primarily governed by its high surface area and mesoporous framework. The porous network provides accessible channels where DBT molecules, despite their bulky polyaromatic structure, can diffuse and become physically trapped within the pores. Additionally, the presence of surface silanol groups (Si–OH) facilitates weak hydrogen bonding or dipole-dipole interactions with the aromatic rings of DBT. While effective, the lack of selective active sites limits the overall sulfur uptake compared to modified versions [23], [28], [29].

2. SiO_2-Ag: Selective Ag–S Affinity and π-Complexation

The incorporation of silver species into the mesoporous silica framework can markedly enhance the selectivity and adsorption strength of SiO_2-Ag toward DBT through the combined contribution of metal–sulfur affinity, π-complexation, and pore-assisted retention. Unlike bare SiO_2, where DBT removal is mainly governed by physical adsorption and weak surface interactions, Ag-modified silica introduces additional chemically active sites in the form of Ag nanoparticles and/or Ag^+ species. These silver sites can directly interact with the sulfur atom of DBT, producing stronger and more selective adsorption through Ag–S coordination [30]. From an electronic interaction perspective, molecular orbital calculations indicate that the lowest unoccupied molecular orbital (LUMO) of Ag species can overlap with the lone-pair electrons of the sulfur atom, facilitating donor–acceptor interaction and stabilizing the adsorbed DBT molecule on the surface [28]. In addition to this sulfur-specific interaction, Ag nanoparticles dispersed on ordered mesoporous silica supports such as MCM-41 or SBA-15 may also interact with the aromatic rings of DBT through π-complexation, which further strengthens molecular retention even when the

https://doi.org/10.66973/jees.26.009

interaction is not exclusively sulfur-selective [31]. Therefore, the enhanced adsorption behavior of SiO_2-Ag can be attributed not only to the accessible mesoporous structure of the silica support, but also to the formation of Ag-associated active centers capable of capturing DBT through multiple interaction pathways. Recent studies on AgO-modified silica further support this mechanism, showing that silver-containing silica adsorbents can achieve significantly higher sulfur removal efficiencies than undoped SiO_2 because chemisorptive Ag–S interactions and aromatic ring stabilization provide stronger binding and improved selectivity toward refractory sulfur compounds [22].

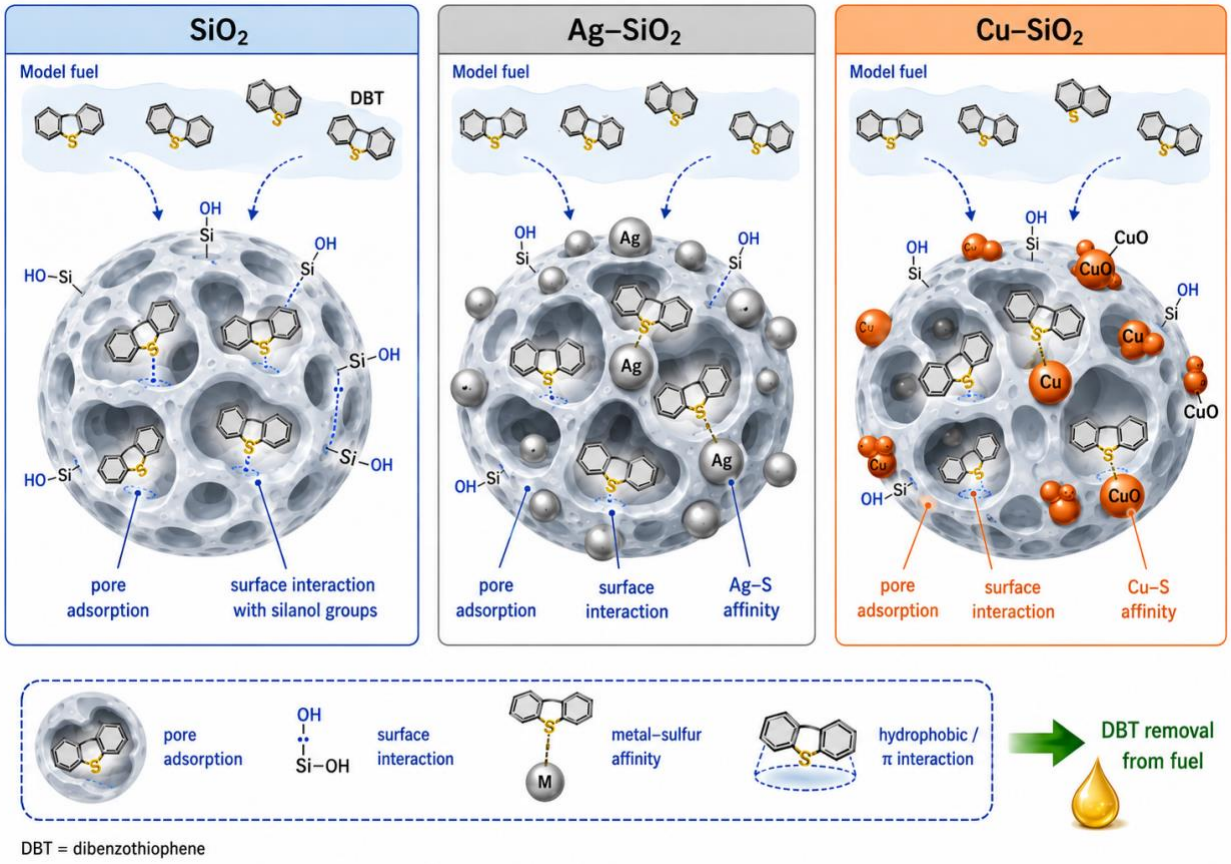

Figure 7. Proposed mechanism for DBT adsorption on SiO_2, Ag–SiO_2, and Cu–SiO_2 nanoparticles

3. SiO_2-Cu: Synergistic Effects of Copper Species

Similarly, SiO_2-Cu utilizes a combination of mesopore filling and Cu–S affinity. Copper species (Cu/CuO or Cu^+) anchored on the silica surface serve as active centers that promote stronger interactions with sulfur-containing compounds [23], [24]. The mesoporous silica framework plays an important role in improving the adsorption performance of SiO_2-Cu by providing a highly porous and spatially confined support that helps disperse copper oxide species and suppresses their aggregation. This structural confinement maintains a high density of accessible Cu-based active sites on the surface and within the pore channels, thereby facilitating the interaction between the adsorbent and DBT molecules [23]. In addition to physical adsorption inside the mesoporous structure, the presence of copper species can introduce stronger and more selective interactions with sulfur-containing compounds. Recent studies on cuprous-loaded mesoporous materials, such as Cu^+-SBA-15, suggest that DBT adsorption is not controlled only

https://doi.org/10.66973/jees.26.009

by pore filling, but is often dominated by chemisorption through Cu–S interactions [24], [32]. The aromatic structure of DBT further strengthens this retention because its conjugated rings can enhance the interaction energy and stabilize the adsorbed molecule near the metal active centers. Therefore, the enhanced DBT removal by Cu-modified silica can be attributed to the combined effect of uniform copper species dispersion, accessible mesoporous channels, strong sulfur–metal affinity, and additional stabilization arising from the aromatic DBT framework.

4. The Role of Aromaticity and Hydrophobicity

DBT is a hydrophobic polyaromatic sulfur compound; its retention is further supported by hydrophobic interactions and weak π-related interactions within confined pore regions. In metal-modified systems, the contribution of selective metal–sulfur binding (Ag–S or Cu–S) becomes the dominant factor, allowing for the deep desulfurization of fuels even in the presence of competing non-sulfur aromatics. This confirms that metal modification is a highly promising strategy for enhancing the efficiency of mesoporous silica in the removal of refractory sulfur compounds like DBT [33].

4 Conclusion

Mesoporous SiO_2, SiO_2–Ag, and SiO_2–Cu nanoparticles were successfully synthesized and characterized for dibenzothiophene adsorption applications. FTIR, XRD and TEM analyses confirmed the formation of highly ordered mesoporous silica structures with spherical morphology and successful deposition of Ag and Cu nanoparticles onto the silica surface. The mesoporous framework remained well preserved after metal incorporation, providing accessible adsorption pathways for DBT molecules.

Adsorption studies revealed distinct adsorption behaviors for pure and metal-decorated silica nanoparticles. SiO_2–Ag and SiO_2–Cu exhibited significantly enhanced initial adsorption rates, indicating that Ag and Cu nanoparticles promoted rapid adsorption through strong interactions with sulfur-containing DBT molecules. However, pure mesoporous SiO_2 demonstrated the highest equilibrium adsorption efficiency, reaching 90.6% after 24 h. This superior performance may be associated with its larger accessible surface area, open pore structure, and reduced pore blockage compared with the metal-decorated samples.

The results suggest that metal decoration improves adsorption kinetics, whereas pure mesoporous silica provides superior long-term adsorption capacity. These findings highlight the important role of pore accessibility and surface chemistry in determining the adsorption performance of mesoporous silica-based nanomaterials for fuel desulfurization and environmental remediation applications.

Funding
This research received no external funding.

Author Contributions
A.K.: Methodology, Software, Writing – Original Draft.
A.O.: Supervision, Conceptualization, Writing – Review & Editing.

Ethics Approval and Consent to Participate
This study did not involve human participants or animals. Therefore, ethical approval and informed consent were not required.

Data Availability Statement
The data supporting the findings of this study are available from the corresponding author upon reasonable request.

Supporting Information
Not applicable.

Conflict of Interest
The authors declare no conflict of interest.

AI Use Disclosure
The authors confirm that No AI tools were used to generate scientific results, data, figures, or interpretations. All analyses, conclusions, and scientific content were developed by the authors.

REFERENCES:

[1] R. B. Engdahl, "A critical review of regulations for the control of sulfur oxide emissions," *Journal of the Air Pollution Control Association*, vol. 23, no. 5, pp. 364–375, 1973, https://doi.org/10.1080/00022470.1973.10469782.
[2] A. Ospanova, A. Ardakkyzy, A. Kurbanova, Y. Kanagat, M. Abutalip, Z. Toktarbay, and N. Nuraje, "Pervaporative desulfurization: A comprehensive review of principles, advances, and applications," *Eurasian Journal of Chemistry*, vol. 28, no. 4, pp. 112–122, 2023, https://doi.org/10.31489/2959-0663/4-23-10.
[3] R. Shafi and G. J. Hutchings, "Hydrodesulfurization of hindered dibenzothiophenes: An overview," *Catalysis Today*, vol. 59, no. 3–4, pp. 423–442, 2000, https://doi.org/10.1016/S0920-5861(00)00308-4.
[4] H. Xiao, H. Zhang, F. Li, and H. Wang, "Mechanisms of dibenzothiophene removal influenced by fuel molecular structure: Carbon chain length, ester groups, unsaturation, and aromaticity," *Fuel*, vol. 390, p. 134708, 2025, https://doi.org/10.1016/j.fuel.2025.134708.
[5] J. C. García-Martínez, G. Chavez-Esquivel, M. M. González-Brambila *et al*., "Temperature effect on quinoline adsorption in dibenzothiophene presence using mesoporous SBA-15 and Zn/SBA-15 materials," *Catalysis Letters*, vol. 154, pp. 2790–2808, 2024, https://doi.org/10.1007/s10562-023-04495-9.
[6] T. O. Ajiboye, A. A. Mafolasire, C. Aruada, O. D. Ogunbiyi, S. Dhibar, and L. N. Nthunya, "Updates on the materials for desulphurization of thiophene, benzothiophene and dibenzothiophene," *Discover Applied Sciences*, vol. 7, no. 5, p. 466, 2025, https://doi.org/10.1007/s42452-025-06604-2.
[7] J. M. Palomino, D. T. Tran, J. L. Hauser, H. Dong, and S. R. Oliver, "Mesoporous silica nanoparticles for high capacity adsorptive desulfurization," *Journal of Materials Chemistry A*, vol. 2, no. 36, pp. 14890–14895, 2014, https://doi.org/10.1039/C4TA02570A.
[8] Y. Shi, G. Liu, and X. Zhang, "Adsorptive removal of dibenzothiophene and dibenzothiophene sulfone over mesoporous materials," *Industrial & Engineering Chemistry Research*, vol. 56, no. 9, pp. 2557–2564, 2017, https://doi.org/10.1021/acs.iecr.6b03673.
[9] S. A. Ganiyu, S. A. Ali, and K. Alhooshani, "Simultaneous HDS of DBT and 4,6-DMDBT over single-pot Ti-SBA-15-NiMo catalysts: Influence of Si/Ti ratio on the structural properties, dispersion and catalytic activity," *RSC Advances*, vol. 7, no. 35, pp. 21943–21952, 2017, https://doi.org/10.1039/C7RA01806A.
[10] J. H. Shan, L. Chen, L. B. Sun, and X. Q. Liu, "Adsorptive removal of thiophene by Cu-modified mesoporous silica MCM-48 derived from direct synthesis," *Energy & Fuels*, vol. 25, no. 7, pp. 3093–3099, 2011, https://doi.org/10.1021/ef200472j.
[11] A. Ospanova, K. Kassym, D. Kanzhigitova, T. Orazbek, A. Ardakkyzy, Z. Toktarbay, and N. Nuraje, "Selective separation of thiophene derivatives using metal–organic frameworks-based membranes," *ACS Omega*, 2024, https://doi.org/10.1021/acsomega.4c05506.
[12] Z. Duan, X. Ding, Y. Wang, L. Zhu, and D. Xia, "A new strategy for fuel desulfurization by molecular inclusion with copper(II)-β-cyclodextrin@SiO_2@Fe_3O_4 for removing thiophenic sulfides," *Energy & Fuels*, vol. 32, no. 11,

pp. 11421–11431, 2018, https://doi.org/10.1021/acs.energyfuels.8b02886.
[13] Z.-C. Kampouraki, D. A. Giannakoudakis, V. Nair, A. Hosseini-Bandegharaei, J. C. Colmenares, and E. A. Deliyanni, "Metal organic frameworks as desulfurization adsorbents of DBT and 4,6-DMDBT from fuels," *Molecules*, vol. 24, no. 24, p. 4525, 2019, https://doi.org/10.3390/molecules24244525.
[14] M. Saeed, A. Riaz, A. Intisar *et al*., "Synthesis, characterization and application of organoclays for adsorptive desulfurization of fuel oil," *Scientific Reports*, vol. 12, p. 7362, 2022, https://doi.org/10.1038/s41598-022-11054-6.
[15] Y. Han, L. Zhang, W. Yang, "Synthesis of Mesoporous Silica Using the Sol–Gel Approach: Adjusting Architecture and Composition for Novel Applications," *Nanomaterials,* vol. 14, no. 11, p. 903, 2024, https://doi.org/10.3390/nano14110903.
[16] M. Song, J. Kim, S. Cho, and J. Kim, "Mixed cationic–nonionic surfactant templating approach for the synthesis of mesoporous silica," *Langmuir*, vol. 18, no. 16, pp. 6110–6115, 2002, https://doi.org/10.1021/la011691v.
[17] T. Aubert, K. Ma, K. Tan, and U. Wiesner, "Two-dimensional superstructures of silica cages," *Advanced Materials*, vol. 32, no. 21, 2020, https://doi.org/10.1002/adma.201908362.
[18] X. Li, H. Zhu, C. Liu, P. Yuan, Z. Lin, J. Yang *et al*., "Synthesis, modification, and application of hollow mesoporous carbon submicrospheres for adsorptive desulfurization," *Industrial & Engineering Chemistry Research*, vol. 57, no. 44, pp. 15020–15030, 2018, https://doi.org/10.1021/acs.iecr.8b02780.
[19] A. Abduraimova *et al*., "Cetyltrimethylammonium bromide (CTAB)-loaded SiO_2–Ag mesoporous nanocomposite as an efficient antibacterial agent," *Nanomaterials*, vol. 11, no. 2, p. 477, 2021, https://doi.org/10.3390/nano11020477.
[20] H. M. Salem, D. Mohmed, and E. G. Zaki, "Nanoarchitectonics of copper tungsten-mesoporous silica with a new template for photo oxidative-desulfurization of dibenzothiophene," *Journal of Inorganic and Organometallic Polymers and Materials*, vol. 32, no. 10, pp. 3725–3737, 2022, https://doi.org/10.1007/s10904-022-02363-4.
[21] P. Tan, J.-X. Qin, X. Liu, X. Yin, and L. Sun, "Fabrication of magnetically responsive core–shell adsorbents for thiophene capture: $AgNO_3$-functionalized Fe_3O_4@mesoporous SiO_2 microspheres," *Journal of Materials Chemistry A*, vol. 2, no. 13, p. 4698, 2014, https://doi.org/10.1039/c3ta14491g.
[22] R. V. Sales *et al*., "Assessment of Ag nanoparticles interaction over low-cost mesoporous silica in deep desulfurization of diesel," *Catalysts*, vol. 9, no. 8, p. 651, 2019, https://doi.org/10.3390/catal9080651.
[23] Y. Yin, W. Jiang, X. Liu, Y. Li, and L. Sun, "Dispersion of copper species in a confined space and their application in thiophene capture," *Journal of Materials Chemistry*, vol. 22, no. 35, p. 18514, 2012, https://doi.org/10.1039/c2jm33216g.
[24] L. Cao *et al*., "Preparation of magnetic hydrophobic Cu+-containing mesoporous materials and their performance in adsorption and removal of organic sulfides from simulated gasoline," *Journal of Environmental Management*, vol. 375, p. 124217, 2025, https://doi.org/10.1016/j.jenvman.2025.124217.
[25] Q. Yao, Z. Lu, Z. Zhang, X. Chen, and Y. Lan, "One-pot synthesis of core-shell Cu@SiO_2 nanospheres and their catalysis for hydrolytic dehydrogenation of ammonia borane and hydrazine borane," *Scientific Reports*, vol. 4, no. 1, 2014, https://doi.org/10.1038/srep07597.
[26] L. Yang, Y. Wang, D. Huang, G. Luo, and D. Youyuan, "Preparation of high performance adsorbents by functionalizing mesostructured silica spheres for selective adsorption of organosulfur compounds," *Industrial & Engineering Chemistry Research*, vol. 46, no. 2, pp. 579–583, 2006, https://doi.org/10.1021/ie061174d.
[27] O. E. Médina *et al*., "Sulfur removal from heavy crude oils based on the adsorption process using CuO- and AgO-modified SiO_2-based nanomaterials: Experimental and theoretical study," *Langmuir*, vol. 41, no. 36, pp. 24683–24700, 2025, https://doi.org/10.1021/acs.langmuir.5c03001.
[28] D. T. Tran, J. M. Palomino, and S. R. J. Oliver, "Desulfurization of JP-8 jet fuel: Challenges and adsorptive materials," *RSC Advances*, vol. 8, no. 13, pp. 7301–7314, 2018, https://doi.org/10.1039/c7ra12784g.
[29] A. Hussain, M. L. McKee, J. M. Heinzel, X. Sun, and B. J. Tatarchuk, "Density functional theory study of organosulfur selective adsorption on Ag–TiO_2 adsorbents," *The Journal of Physical Chemistry C*, vol. 118, no. 27, pp. 14938–14947, 2014, https://doi.org/10.1021/jp503097y.
[30] S. G. McKinley and R. J. Angelici, "Deep desulfurization by selective adsorption of dibenzothiophenes on Ag+/SBA-15 and Ag+/SiO_2," *Chemical Communications*, no. 20, p. 2620, 2003, https://doi.org/10.1039/b309249f.
[31] E. R. Webster *et al*., "Adsorption of dibenzothiophene and fluorene on TiO_2(110) and supported Ag clusters," *E*

nergy & Fuels, vol. 27, no. 11, pp. 6575–6580, 2013, https://doi.org/10.1021/ef401581x.
[32] Y. X. Li *et al*., "Enhancing oxidation resistance of Cu(I) by tailoring microenvironment in zeolites for efficient adsorptive desulfurization," *Nature Communications*, vol. 11, Art. no. 3206, 2020, https://doi.org/10.1038/s41467-020-17042-6.
[33] R. T. Yang, A. J. Hernández-Maldonado, and F. H. Yang, "Desulfurization of transportation fuels with zeolites under ambient conditions," *Science*, vol. 301, no. 5629, pp. 79–81, 2003, https://doi.org/10.1126/science.1085088.